BJP British Journal of Pharmacology

DOI:10.1111/bph.13223
www.brjpharmacol.org

RESEARCH PAPER

Genetic predisposition to albuminuria is associated with increased arterial stiffness: role of elastin

Correspondence
María S. Fernández-Alfonso, Instituto Pluridisciplinar, Universidad Complutense, Paseo Juan XXIII, 1. 28040 Madrid, Spain. E-mail: marisolf@farm.ucm.es

Received
23 December 2014
Revised
8 June 2015
Accepted
10 June 2015

M Gil-Ortega[1], C F García-Prieto[1], G Ruiz-Hurtado[2,3], C Steireif[2,4], M C González[5], A Schulz[4], R Kreutz[4], M S Fernández-Alfonso[2], S Arribas[5] and B Somoza[1]

[1]*Departamento de Ciencias Farmacéuticas y de la Salud, Facultad de Farmacia, Universidad CEU – San Pablo, Madrid, Spain,* [2]*Instituto Pluridisciplinar and Facultad de Farmacia, Universidad Complutense, Madrid, Spain,* [3]*Instituto de Investigación imas12, Hospital Universitario 12 de Octubre, Madrid, Spain,* [4]*Department of Clinical Pharmacology and Toxicology, Charité – Universitätsmedizin, Berlin, Germany, and* [5]*Departamento de Fisiología, Universidad Autónoma, Madrid, Spain*

BACKGROUND AND PURPOSE

The Munich Wistar Frömter (MWF) rat strain represents an experimental model to study cardiovascular alterations under conditions of progressive albuminuria. The aim of this study was to evaluate the association between genetic predisposition to albuminuria and the development of arterial stiffness and/or vascular remodelling.

EXPERIMENTAL APPROACH

Experiments were performed in mesenteric arteries from 12-week-old MWF, Wistar Kyoto (WKY) and consomic MWF-6^{SHR} and MWF-8^{SHR} rats in which chromosomes 6 or 8 associated with albuminuria from MWF were replaced by the respective chromosome from spontaneously hypertensive rats (SHR).

KEY RESULTS

Incremental distensibility, wall stress and strain were reduced, and arterial stiffness was significantly increased in albuminuric MWF compared with WKY. Albuminuria suppression in both consomic strains was associated with lower β-values in MWF-8^{SHR} and MWF-6^{SHR} compared with MWF. Moreover, elastin content was significantly lower in MWF external elastic lamina compared with WKY and both consomic strains. In addition, a reduction in arterial external and internal diameter and cross-sectional area was detected in MWF compared with WKY, thus exhibiting an inward hypotrophic remodelling. However, these alterations remained unchanged in both consomic strains.

CONCLUSION AND IMPLICATIONS

These data demonstrate that albuminuria in MWF is associated with increased arterial stiffness due to a reduction of elastin content in the external elastic lamina. Moreover, inward hypotrophic remodelling in MWF is not directly associated with albuminuria. In contrast, we demonstrated that two major genetic loci affect both the development of albuminuria and arterial stiffness, thus linking albuminuria and impairment of mechanical properties of resistance arteries.

Abbreviations

CKD, chronic kidney disease; D_{e0Ca}, external diameter; D_{i0Ca}, internal diameter; EEL, external elastic laminae; E_{max}, maximal response; IEL, internal elastic laminae; KH, Krebs–Henseleit solution; MA, superior mesenteric artery; MRA, mesenteric resistance arteries; MWF, Munich Wistar Frömter; QTL, quantitative trait loci; RNO, rat chromosome; SBP, systolic BP; SHR, spontaneously hypertensive rats; UAE, urinary albumin excretion; WKY, Wistar Kyoto; WT, Wall thickness

Tables of Links

TARGETS
Endothelial NOS

LIGANDS	
ACh	L-NAME
	NA

These Tables list key protein targets and ligands in this article which are hyperlinked to corresponding entries in http://www.guidetopharmacology.org, the common portal for data from the IUPHAR/BPS Guide to PHARMACOLOGY (Pawson *et al.*, 2014) and are permanently archived in the Concise Guide to PHARMACOLOGY 2013/14 (Alexander *et al.*, 2013a).

Introduction

Increased urinary albumin excretion (UAE) is an early marker of renal and vascular damage (Deckert *et al.*, 1989; Gansevoort *et al.*, 2010; Matsushita *et al.*, 2010). It is an independent risk factor predicting the development of cardiovascular and renal complications in patients with essential hypertension or diabetes, and also in the general population (Fogarty *et al.*, 2000; Krolewski *et al.*, 2006; Freedman *et al.*, 2008; Gschwend *et al.*, 2009; Cerezo *et al.*, 2012). A common pathway linking the cardiovascular–renal axis in microalbuminuric patients might be a generalized and systemic vascular dysfunction due to structural and functional alterations (Mottl *et al.*, 2009; Divers and Freedman, 2010; Schulz and Kreutz, 2012a).

Vascular dysfunction in albuminuric patients (Hermans *et al.*, 2007; 2008) and in patients with chronic kidney disease (CKD) (Schiffrin *et al.*, 2007) has been associated with an increased oxidative stress in the glomeruli and in the vascular wall (Vaziri *et al.*, 2002; Satoh, 2012). Moreover, albuminuria breakthrough in patients in early stages of CKD under chronic renin-angiotensin-system blockade is accompanied by an amplified oxidative damage, which is not well compensated by a sufficient endogenous antioxidant defence (Ruiz-Hurtado *et al.*, 2014). Munich Wistar Frömter (MWF) rats, an experimental genetic model of progressive albuminuria development with an inherited nephron deficit (Schulz *et al.*, 2003; 2008), show impaired endothelium-dependent relaxation in coronary microvessels (Gschwend *et al.*, 2002), mesenteric arteries (Gschwend *et al.*, 2002) and in the aorta (Ulu *et al.*, 2009; Szymanski *et al.*, 2012). In this model, endothelial dysfunction is related to a decrease in NO bioavailability linked to an enhanced superoxide anion (O_2^-) production (Steireif *et al.*, 2013). Genetic introgression of rat chromosome (RNO) 8 (RNO8) from the spontaneously hypertensive rat (SHR), as a contrasting model of hypertension with low-grade albuminuria, into the MWF background (MWF-8^{SHR}) significantly suppressed albuminuria and completely restored endothelial function together with the abnormal O_2^- production in aortic rings (Steireif *et al.*, 2013).

Several studies have reported the association between albuminuria and arterial stiffness in hypertensive (Mule *et al.*, 2004; Munakata *et al.*, 2009) and diabetic patients (Yokoyama *et al.*, 2004; Smith *et al.*, 2005; Bouchi *et al.*, 2011; Hashimoto and Ito, 2011), as well as in the general population (Kohara *et al.*, 2004; Ishikawa *et al.*, 2008). Epidemiological data indicate an independent association between albuminuria and arterial stiffness in both normotensive and non-diabetic individuals, suggesting the possibility of a similar pathophysiological mechanism involved in these two indices of subclinical target organ damage (Kim *et al.*, 2011). Moreover, albuminuria has also been associated with maladaptive carotid remodelling characterized by a greater circumferential wall stress (Szymanski *et al.*, 2012).

A link between endothelial dysfunction leading to arterial stiffness has been proposed (Wilkinson *et al.*, 2002). Concurrently, the increase in pulsatile mechanical load induced by arterial stiffness could further damage the endothelium, which in turn could induce microalbuminuria, thus starting a vicious cycle leading to reduced vessel elasticity and hypertension (Munakata *et al.*, 2009). We hypothesized that the analysis of the MWF strain and its derived consomic MWF-6^{SHR} and MWF-8^{SHR} strains, in which the MWF chromosomes RNO6 and RNO8 have been replaced by the corresponding SHR chromosomes, might provide mechanistic insights into the link between albuminuria and arterial stiffness. The aim of this study was, therefore, to evaluate the relationship between albuminuria and alterations in vascular structure and mechanics of mesenteric resistance arteries (MRAs) in MWF rats. We further tested whether suppression of albuminuria development in consomic MWF-6^{SHR} and MWF-8^{SHR} by exchange of two chromosomes that carry major albuminuria quantitative trait loci (QTL) (Schulz *et al.*, 2007; 2012b) affects these vascular parameters.

Methods

Animals

Parental MWF (MWF/FubRkb) and consomic MWF-6^{SHR} (MWF-Chr 6^{SHR}/Rkb) and MWF-8^{SHR} (MWF-Chr 8^{SHR}/Rkb) animals (n = 5–10 per strain) were obtained from our colonies (laboratory code Rkb; http://dels.nas.edu/ilar/) at the Charité – Universitätsmedizin Berlin, Germany. The development of the MWF-6^{SHR} and MWF-8^{SHR} consomic strains has been previously reported (Schulz *et al.*, 2007; 2008). Twelve-week-old male rats were housed under controlled light (12 h light/dark cycles from 08:00 to 20:00 h) and temperature (22–24°C) conditions with standard water and food *ad libitum*. Although the comparative analysis between MWF and consomic strains was the main focus of this study, an additional group of n = 5–10 Wistar Kyoto (WKY) rats (purchased from Charles River, Barcelona, Spain) was used as a control strain with both normal blood pressure and normal (or low-grade) albuminuria. We have also included a group of SHRs (n = 5) as a control model for vascular eutrophic inward remodelling and arterial stiffness (Supporting Information Figs. S1–S5). The Institutional Animal Care and Use Committee approved all experimental procedures according to the guidelines for ethical care of experimental animals of the European Community, and all efforts were made to avoid animal suffering. All studies involving animals are reported in accordance with the ARRIVE guidelines for reporting experiments involving animals (Kilkenny *et al.*, 2010; McGrath *et al.*, 2010).

Laboratory measurements

For urine analysis, animals were placed in metabolic cages for 2 days. After 1 day of adaptation, urine was collected for 24 h for UAE analysis measured with a rat-specific ELISA technique (Steireif *et al.*, 2013). Systolic BP (SBP) was assessed by tail-cuff measurements in awake rats as previously described (Kreutz *et al.*, 2000). Animals were killed by decapitation and superior mesenteric arteries (MA), and third-order MRAs were quickly dissected, immersed in oxygenated Krebs solution and cleaned of blood by gentle shaking. MRA was used to study structure and mechanic properties (pressure myography) and elastin content. MA was used to study vascular function (organ bath). Basal O_2^- availability was determined by confocal microscopy in third-order MA branches with dihydroethidium (DHE; 3 μM) and quantified as previously described (Gonzalez *et al.*, 2008; Gil-Ortega *et al.*, 2014).

Structural and mechanical properties in mesenteric arteries

MRA of 12-week-old rats was studied by pressure myography (Model P100, Danish Myo-Tech, Aarhus, Denmark) as previously described (Briones *et al.*, 2003; Conde *et al.*, 2011). Briefly, MRA segments (2–3 mm) were placed on two glass cannulas and tied with surgical nylon suture. Cannulas were separated so that vessel walls were parallel without stretch. Thereafter, intraluminal pressure was set at 70 mmHg for 60 min to equilibrate MRA segments, incubated at 37°C and bubbled with a mixture of 95% O_2 and 5% CO_2 in calcium-free Krebs–Henseleit solution (0 Ca^{2+}-KH; in mmol·L^{-1}: 115 NaCl, 4.6 KCl, 25 $NaHCO_3$, 1.2 KH_2PO_4, 1.2 $MgSO_4$, 10 EGTA and 5.5 glucose), which allowed the determination of vascular structure and mechanics without the influence of vessel tone. External and internal diameters (D_{e0Ca} and D_{i0Ca}, respectively) were recorded at each intraluminal pressure level (3, 20, 40, 60, 80, 100, 120 and 140 mmHg) with a video camera coupled to Myoview software (Danish Myo-Tech). Afterwards, MRA segments were fixed at 70 mmHg with 4% paraformaldehyde (in 0.2 mol·L^{-1} phosphate buffer, pH 7.2–7.4) at 37°C for 45 min and stored at 4°C for confocal microscopy studies.

The following structural and mechanical parameters were calculated using D_{e0Ca} and D_{i0Ca} values: wall thickness, WT = $(D_{e0Ca} - D_{i0Ca})/2$; cross-sectional area = $(\pi/4) \times (D_{e0Ca}^2 - D_{i0Ca}^2)$; wall : lumen ratio = $(D_{e0Ca} - D_{i0Ca})/2D_{i0Ca}$; incremental distensibility = $\Delta D_{i0Ca}/(D_{i0Ca} \times \Delta P) \times 100$; circumferential wall strain (ε) = $(D_{i0Ca} - D_{00Ca})/D_{00Ca}$, where D_{00Ca} is the diameter at 3 mmHg and D_{i0Ca} is the observed internal diameter for a given intravascular pressure in 0 Ca^{2+} KH; circumferential wall stress (β) = $(P \times D_{i0Ca})/(2WT)$, where P is the intraluminal pressure (1 mmHg = 1.334 dynes cm^{-2}) and WT is wall thickness at each intraluminal pressure in 0 Ca^{2+} KH. The β-parameter, obtained from the stress–strain relationship, is proportional to Young's increased elastic modulus and was used to evaluate the intrinsic arterial stiffness independently of vessel geometry (Dobrin, 1978).

Elastin content and organization in mesenteric arteries

Elastin content was determined in external (EEL) and internal elastic lamina (IEL) of previously fixed MRA by confocal microscopy as described in Briones *et al.* (2003). Briefly, MRA segments were mounted intact with fluoroguard (glycerol-antifade agent; Bio-Rad, Hercules, CA, USA) mounting medium on slides containing small wells to avoid artery deformation. Based on elastin autofluorescent properties, MRA segments were visualized with a Leica TCS SP5 confocal microscope (Leica Microsystems, Heidelberg, Germany) (excitation wavelength 488 nm/emission wavelength 500–560 nm). Serial optical sections were captured with a ×63 oil immersion objective, from the adventitia to the lumen. All images were taken under identical conditions of laser intensity, brightness and contrast. Quantitative analyses were performed with three randomly selected regions of EEL and IEL of at least five independent experiments using Metamorph Images Analysis Software (Universal Imaging Corporation, Buckinghamshire, UK) as described in Briones *et al.* (2003). From each stack of serial images, individual projections of the adventitia, external elastic lamina (EEL) and IEL were reconstructed. From EEL and IEL projections, several measurements were obtained as follows. Fluorescence intensity of elastin (average fluorescent intensity per pixel) was measured in several regions (minimum of 5) of the projection and averaged. The amount of elastin in the IEL was quantified from the average fluorescence intensity per pixel. Projections of both EEL and IEL were reconstructed and total fenestrae number, fenestra area, relative area occupied by elastin in EEL and elastin content in IEL were calculated.

Vascular function in mesenteric arteries

MA was carefully isolated, placed in oxygenated KH (115 mmol·L^{-1} NaCl, 4.6 mmol·L^{-1} KCl, 2.5 mmol·L^{-1} $CaCl_2$, 25 mmol·L^{-1} $NaHCO_3$, 1.2 mmol·L^{-1} KH_2PO_4, 1.2 mmol·L^{-1}

Table 1

Characterization of 12-week-old WKY, MWF and consomic MWF-6^{SHR} and MWF-8^{SHR} rats

Phenotype	WKY	MWF	MWF-6^{SHR}	MWF-8^{SHR}
Body weight (g)	282.4 ± 4.9	302.6 ± 4.3	311.2 ± 15.8*	313.2 ± 6.1*
UAE (mg 24 h^{-1})	0.2 ± 0.1	46.2 ± 4.0*	2.5 ± 0.4$^{\&}$	4.8 ± 0.6$^{\&}$
SBP (mmHg)	139 ± 5	146 ± 1	151 ± 2	156 ± 2*,$^{\&\&}$

Phenotype values are means ± SEM. *P < 0.05 compared with WKY; $^{\&}P$ < 0.05 and $^{\&\&}P$ < 0.01 compared with MWF.

$MgSO_4$, 0.01 mmol·L^{-1} EDTA and 5.5 mmol·L^{-1} glucose), cleaned of blood and perivascular fat, and cut into 3 mm long segments. MA segments were suspended on two intraluminal parallel wires, introduced in an organ bath with oxygenated KH, connected to a Piodem strain gauge for isometric tension recording and given an optimal resting tension of 1.5 g. This tension was readjusted every 15 min during an equilibration period of 90 min. Afterwards, segments were incubated with 75 mmol·L^{-1} KCl to check their contractility, and concentration–response curves to ACh (10^{-9}–10^{-4} mol·L^{-1}) were performed in segments previously contracted with noradrenaline (NA; 10^{-7} mol·L^{-1}). Because no differences were observed in the contractile response to NA between strains or treatments, we used the same concentration in all experiments. Tissues were pre-incubated in N^{G}-nitro-L-arginine methyl ester (L-NAME; 10^{-4} mol·L^{-1}) for 20 min.

Materials

ACh was dissolved in saline. NA was dissolved in 0.01% ascorbic acid/saline. L-NAME was dissolved in distilled water. DHE was dissolved in DMSO and was kept in the dark under argon. ACh, L-NAME and DHE were obtained from Sigma-Aldrich (Madrid, Spain). The drug/molecular target nomenclature conforms to BJP's Concise Guide to Pharmacology (Alexander *et al.*, 2013a,b).

Statistical analysis

Data are expressed as mean ± SEM of n independent experiments. Statistical analyses were performed with Stat View software (SAS Institute, Cary, NC, USA). Statistical significance was analysed with one-way ANOVA followed by a Newman–Keuls *post hoc* test and was set at P < 0.05. EC_{50} values as potency indication are expressed as –log EC_{50} (pD_2) and E_{max} values as maximal response. The inhibitory effect of L-NAME on ACh-induced relaxation was quantified from AUC calculated from the individual concentration–response curve plots (GraphPad Software, La Jolla, CA, USA).

Results

MWF, in comparison with the WKY strain, exhibited significantly higher UAE (Table 1). Transfer of RNO6 or RNO8 from SHR into the MWF genetic background resulted in a significant suppression of UAE in both consomic MWF-6^{SHR} and MWF-8^{SHR} compared with MWF (Table 1). WKY, MWF-6^{SHR} and MWF-8^{SHR} animals demonstrated overall UAE values in the low-grade range and no statistical difference between groups. Both MWF and MWF-6^{SHR} exhibited similar SBP values than WKY, but a small increase in SBP was detected in MWF-8^{SHR} animals compared with WKY (Table 1).

Endothelial-dependent response

Relaxation to ACh (10^{-9}–10^{-4} mol·L^{-1}) in mesenteric artery rings (MA) from MWF was significantly impaired (P < 0.001) and associated with a significant reduction in E_{max} and potency (PD_2) values (Table 2) compared with WKY (Figure 1A), but similar to SHR (Supporting Information Fig. S1). Relaxation to ACh was significantly improved in the consomic MWF-8^{SHR} strain (Figure 1A and Table 2) being similar in E_{max} and pD_2 values to WKY. In MWF-6^{SHR}, pD_2 value of ACh was significantly different from MWF and similar to WKY, although E_{max} was similar to MWF (Figure 1A).

The relative contribution of endothelial factors involved in ACh-induced relaxation was analysed separately in each strain (Figure 1B–E).

The contribution of NO in response to ACh was analysed in the presence of the NOS inhibitor, L-NAME (10^{-4} mol·L^{-1}). Endothelial relaxation was significantly reduced by L-NAME in all four strains, although with quantitative differences. L-NAME nearly abolished relaxation to ACh in WKY (Figure 1B), whereas its inhibitory effect was significantly lower in MWF (Figure 1C; P < 0.05). The effect of L-NAME in MWF-6^{SHR} rats was similar to MWF (Figure 1D), whereas in MWF-8^{SHR} it was similar to WKY (Figure 1E). Quantification of the inhibitory effect of L-NAME on ACh-induced relaxation (Figure 1F), which indirectly reflects contribution of NO, showed a reduced effect for both MWF and MWF-6^{SHR}, whereas it showed a major contribution of NO to ACh-induced relaxation in WKY and MWF-8^{SHR}.

Arterial structure

External and internal diameters were significantly reduced at the entire range of pressures (3–140 mmHg) in MWF compared with WKY (P < 0.001; Figure 2A and B). No differences were observed in WT (Figure 2C), whereas wall-to-lumen ratio was significantly higher (Figure 2D; P < 0.01) and cross-sectional area was smaller (Figure 2E; P < 0.05) in MWF in comparison with WKY. Thus, MRA from MWF demonstrated an inward hypotrophic remodelling phenotype compared with WKY (Figure 2F) in contrast to the inward eutrophic remodelling exhibited by SHR (Figures 2F and Supporting Information Fig. S2). All structural parameters in MWF-6^{SHR} and MWF-8^{SHR} were similar to MWF (Figure 2A–F).

Table 2

Efficacy (E_{max}), pD_2 and AUC of ACh in mesenteric arteries of 12-week-old MWF, WKY rats and consomic MWF-6^{SHR} and MWF-8^{SHR} rats

	WKY	MWF	MWF-6^{SHR}	MWF-8^{SHR}
E_{max}				
Control	96.7 ± 1.6	80.5 ± 2.0***	79.9 ± 2.4***	92.2 ± 2.3$^{\&\&}$
L-NAME	7.0 ± 0.8	40.5 ± 9.2*	17.6 ± 5.0$^{\&}$	12.9 ± 9.0
pD_2				
Control	7.0 ± 0.1	6.1 ± 0.1**	6.8 ± 0.1$^{\&\&\&}$	6.7 ± 0.1$^{\&\&}$
L-NAME	5.2 ± 0.6	5.3 ± 0.2	6.0 ± 0.2$^{\&}$	5.3 ± 0.1
AUC				
Control	310.4 ± 16.4	195.5 ± 11.28***	233.7 ± 7$^{\&}$	278.0 ± 7.4$^{\&}$
L-NAME	24.1 ± 3.5	47.8 ± 11.5*	35.5 ± 6.8	30.0 ± 12.8

Values are expressed as means ± SEM. *P < 0.05, **P < 0.01 and ***P < 0.001 compared with WKY; $^{\&}P$ < 0.05, $^{\&\&}P$ < 0.01 and $^{\&\&\&}P$ < 0.001 compared with MWF.

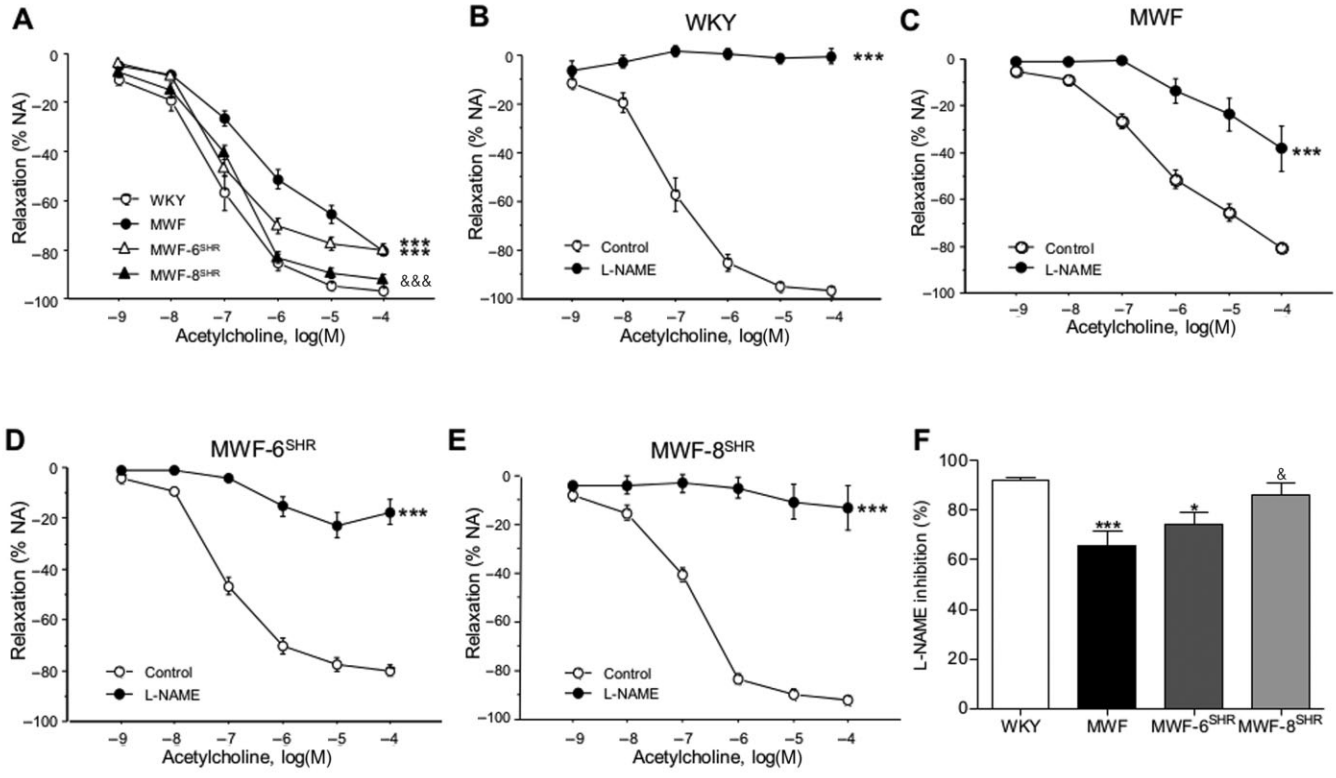

Figure 1

Characterization of endothelial function in an organ bath and endothelial factor contribution to ACh-induced relaxation. (A) Cumulative concentration–response curves to ACh (10^{-9}–10^{-4} mol·L^{-1}) in MA from WKY, MWF, consomic MWF-6^{SHR} and consomic MWF-8^{SHR} rats. Data are means ± SEM (n = 5 animals per group). ***P < 0.001 compared with WKY and $^{\&\&\&}P$ < 0.001 compared with MWF. (B–E) Effect of L-NAME (10^{-4} M) on ACh-induced relaxation in mesenteric arteries from (B) WKY, (C) MWF, (D) MWF-6^{SHR} and (E) MWF-8^{SHR} rats. ***P < 0.001 compared with control relaxation. (F) Bars show quantification of the inhibitory effect of L-NAME on ACh-induced relaxation. Data are means ± SEM (n = 5 animals per group). *P < 0.05 and ***P < 0.001 compared with WKY; $^{\&}P$ < 0.05 compared with MWF.

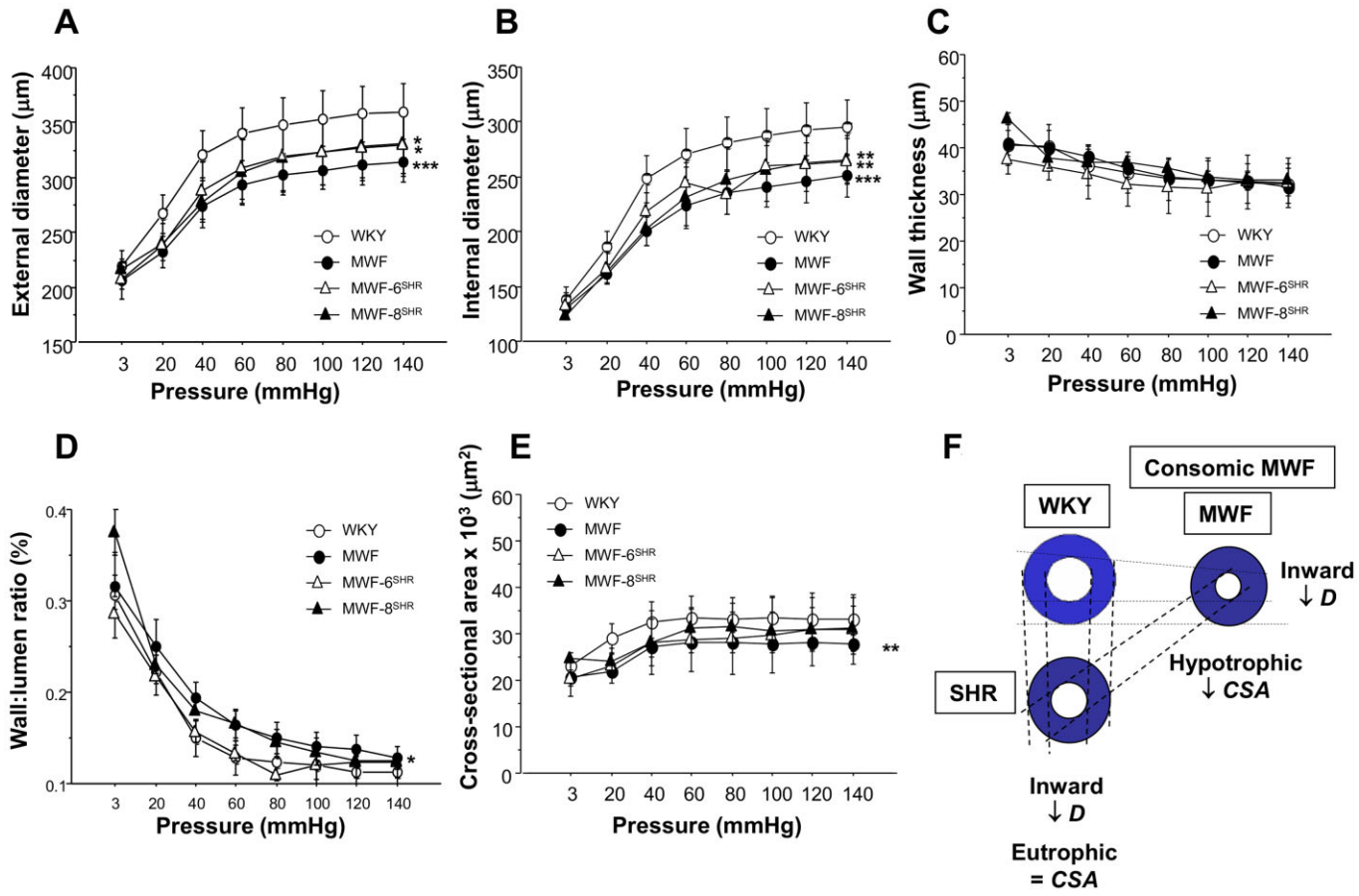

Figure 2

Characterization of structural parameters by pressure myography. (A) External diameter–pressure, (B) internal diameter–pressure and (C) WT–pressure curves in MA from WKY, MWF, MWF-6^{SHR} and MWF-8^{SHR} rats incubated in Ca^{2+}-free KH. Results are expressed as mean ± SEM of n = 5. *P < 0.05, **P < 0.01 and ***P < 0.001 compared with WKY. (D) Wall-to-lumen ratio–pressure and (E) and cross-sectional area–pressure curves in MA from WKY, MWF, MWF-6^{SHR} and MWF-8^{SHR} rats incubated in Ca^{2+}-free KH. Results are expressed as mean ± SEM of n = 5. *P < 0.05 and **P < 0.01 MWF compared with WKY. (F) Scheme showing vascular remodelling patterns in MA from WKY, MWF, MWF-8^{SHR}, MWF-6^{SHR} and SHR rats.

Arterial mechanics

Incremental distensibility was significantly reduced in MRA from MWF only at low-pressure values (20 and 40 mmHg) compared with MRA from WKY rats (Figure 3A; P < 0.05). In MRA from both consomic MWF-6^{SHR} and MWF-8^{SHR}, incremental distensibility values were higher and similar to those obtained in WKY (Figure 3A).

Wall stress and strain were significantly lower in MRA from MWF at all intraluminal pressures (3–140 mmHg) compared with MRA from WKY (Figure 3B; P < 0.01 and Figure 3C; P < 0.001). In consomic MWF-6^{SHR} and MWF-8^{SHR} rats, wall stress and strain significantly increased as compared with MWF being similar to WKY (Figure 3B and C respectively).

MRA from MWF also exhibited an increased intrinsic stiffness compared with WKY as shown by the leftward shift of the stress–strain relationship and the significantly larger β-values compared with WKY (Figure 3D; P < 0.05), but to a similar extent than SHR (Supporting Information Fig. S3). The stress–strain relationship was shifted towards the right in MRA from both consomic MWF-6^{SHR} and MWF-8^{SHR}, and β-values were significantly lower compared with MWF rats (Figure 3D, MWF-6^{SHR}; P < 0.01; MWF-8^{SHR}; P < 0.05). Stiffness index β-values from consomic MWF rats and WKY did not differ statistically.

Elastin content

Elastin content in EEL (Figure 4A and C) and IEL (Figure 4B and D) was significantly lower in MWF compared with both WKY (P < 0.001 and P < 0.01, respectively) and SHR (Supporting Information Fig. S4A–D; P < 0.01 and P < 0.05 respectively). In addition, elastin organization in the IEL was altered in MWF exhibiting significantly smaller fenestrae than WKY (Figure 4B and E; P < 0.05) and SHR (Supporting Information Fig. S4E) without changes in their number (Figure 4F). In both consomic rats, elastin content in EEL was higher than in MWF (Figure 4C; P < 0.01) but lower than in WKY rats (Figure 4C; P < 0.05). No changes were observed in IEL (elastin content, area or number of fenestrae) compared with MWF (Figure 4E and F).

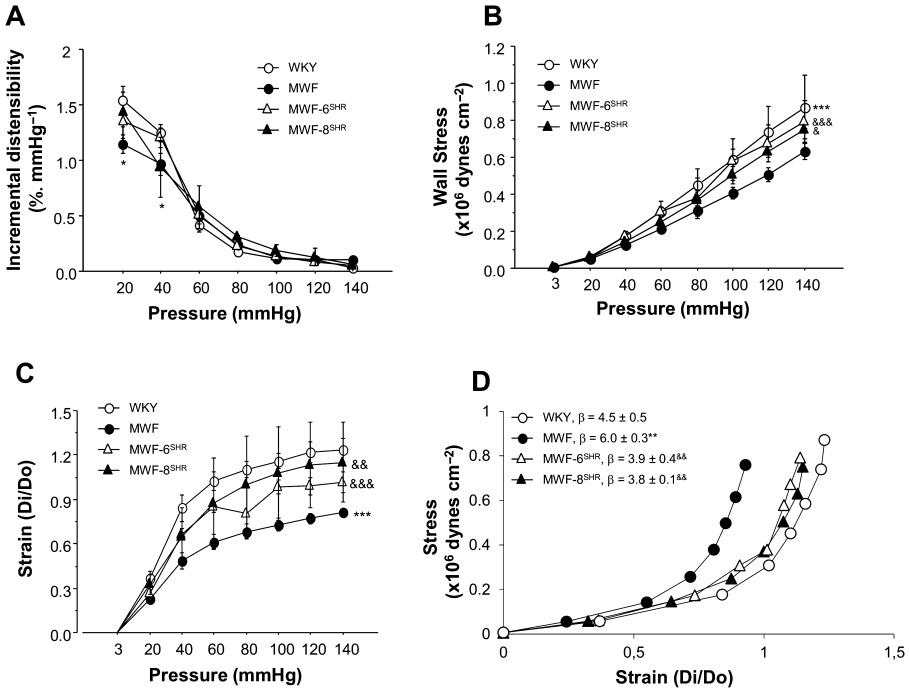

Figure 3

Characterization of mechanical parameters by pressure myography. (A) Incremental distensibility–pressure curve, (B) wall stress–pressure curve, (C) strain–pressure curve and (D) stress–strain relationships with β-values obtained from fully relaxed (Ca^{2+}-free KH) MA segments from WKY, MWF, MWF-6^{SHR} and MWF-8^{SHR} rats calculated from pressure myography data. Data are expressed as mean ± SEM of $n = 5$. *$P < 0.05$, **$P < 0.01$ and ***$P < 0.001$ compared with WKY. $^{\&}P < 0.05$, $^{\&\&}P < 0.01$ and $^{\&\&\&}P < 0.001$ compared with MWF.

Superoxide anion levels in third-order mesenteric arteries

Superoxide anion availability (Figure 5A and B) in MWF MAs was significantly higher compared with WKY ($P < 0.05$) but similar to SHR (Supporting Information Fig. S5). However, both consomic MWF-6^{SHR} and MWF-8^{SHR} exhibited normal levels, thus being similar to WKY.

Discussion

In the present study, we showed that spontaneous albuminuria in MWF rats is associated with increased arterial stiffness and with a reduction in elastin content in the EEL. Moreover, we demonstrated for the first time a genetic link between albuminuria development and increased arterial stiffness, as separate transfer of RNO6 or RNO8 from SHR into the MWF background significantly diminishes both albuminuria and arterial stiffness. MWF rats also exhibited an inward hypotrophic remodelling in MRA, which was, however, not directly associated with albuminuria development as it was not reversed in consomic MWF-6^{SHR} and MWF-8^{SHR} rats.

A previous study in humans shows the association between albuminuria and arterial stiffness determined by pulse wave velocity in non-hypertensive and non-diabetic conditions (Kim *et al.*, 2011). Similarly, albuminuria has also been related to arterial stiffness in several studies performed in patients with hypertension (Mule *et al.*, 2004; Munakata *et al.*, 2009) or with type 2 diabetes (Yokoyama *et al.*, 2004; Smith *et al.*, 2005; Bouchi *et al.*, 2011; Huang *et al.*, 2014; Sjoblom *et al.*, 2014). Consequently, albuminuria has been suggested as an early marker for the detection of arterial stiffness in those patients (Huang *et al.*, 2014). In accordance with these findings, MRA from MWF rats exhibited reduced increased distensibility, wall stress and strain and, consequently, an increased arterial stiffness determined by the β-value of the stress–strain relationship. One crucial determinant of mechanical properties of the vascular wall is elastin. Changes in its content and organization have been shown to compromise arterial elasticity, thus contributing to increase arterial stiffness (Intengan *et al.*, 1999). Our group has previously reported that the reduction in incremental distensibility at low pressures is related to changes in both elastin content and/or elastin organization (Briones *et al.*, 2003). In fact, MWF show a significant reduction in elastin content in both EEL and IEL together with a reduction of IEL fenestrae area associated with a reduced increased distensibility at 20 and 40 mmHg. In addition, the reduction of fenestrae size might compromise mechanical properties (Arribas *et al.*, 2008) as there is a positive correlation between IEL fenestrae size and β-values (Gonzalez *et al.*, 2005; 2006).

As a limitation of the current study, we did not determine plasma markers of kidney function. However, previous studies demonstrated that plasma levels of creatinine or creatinine clearance levels are not different between MWF, normotensive or SHR adult animals up to the age of 24 weeks

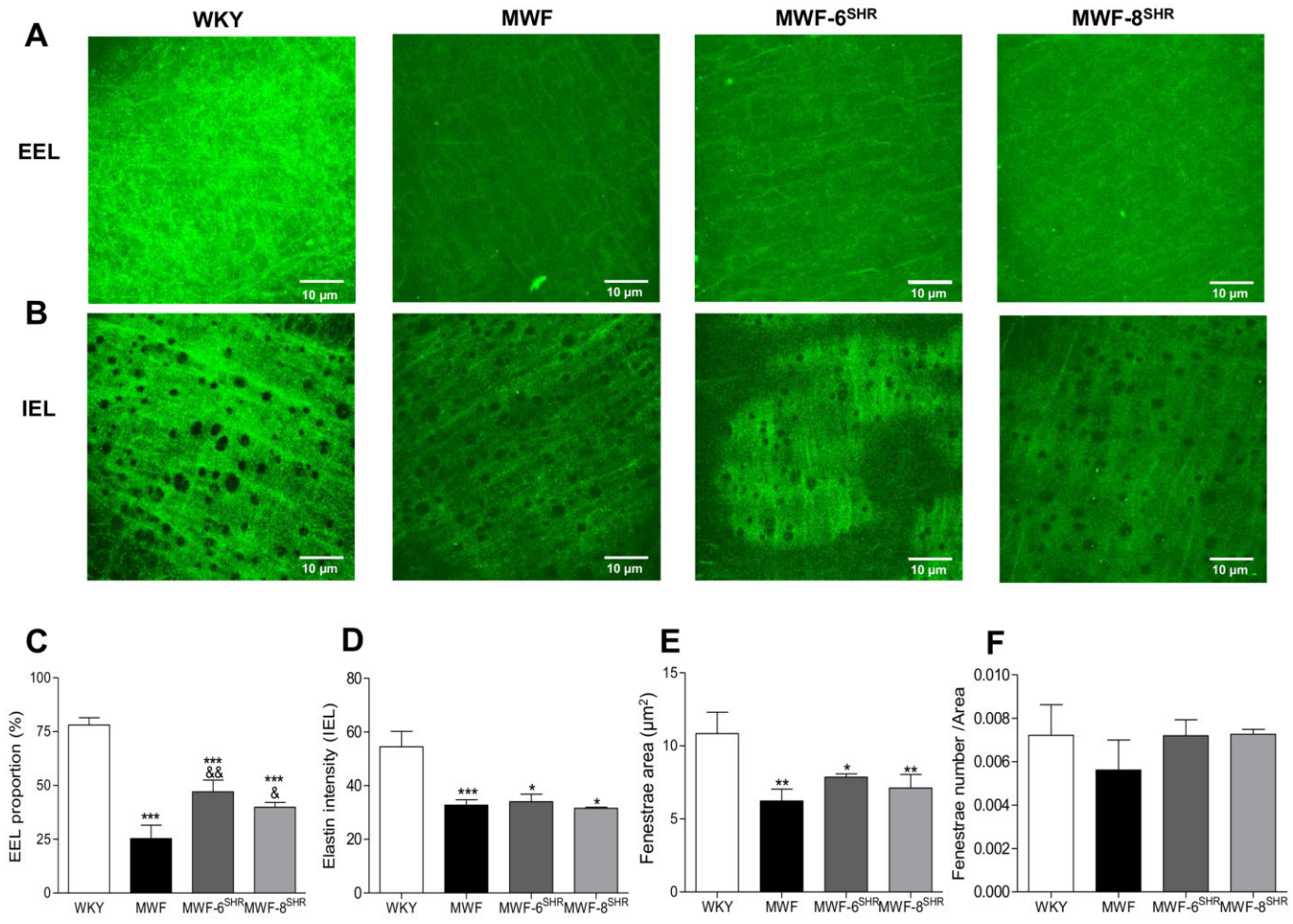

Figure 4

Determination of elastin content and organization. Representative confocal projections of the EEL (A) and IEL (B) of MA from WKY, MWF, MWF-6^{SHR} and MWF-8^{SHR}. Projections were obtained from serial optical sections captured with a fluorescence confocal microscope (×63 oil immersion objective, zoom ×2). Bars show quantification of elastin proportion in EEL (C) and elastin content in IEL (D), fenestrae size (E) and fenestrae number (F). Results are expressed as mean ± SEM of $n = 5$. *$P < 0.05$, **$P < 0.01$ and ***$P < 0.001$ compared with WKY. $^{\&}P < 0.05$ and $^{\&\&}P < 0.01$ compared with MWF.

(Schulz *et al.*, 2002; 2007). Thus, although MWF rats inherit a nephron deficit they compensate for this by increasing their single nephron glomerular filtration rate (Fassi *et al.*, 1998), and thereby maintain a normal global renal function in terms of glomerular filtration rate in young adult animals as studied in this report.

Consomic MWF-8^{SHR} and MWF-6^{SHR} strains have been useful experimental tools to verify the role of albuminuria in endothelial dysfunction. In this regard, we have recently reported that endothelial function, which is significantly compromised in aortas from MWF rats, is completely restored in consomic MWF-8^{SHR} due to an increase in NO availability, probably related to smaller superoxide anion levels. In contrast, introgression of RNO6 into the MWF background had no effect on either endothelial dysfunction or NO availability (Steireif *et al.*, 2013). In the present study, we showed similar results in MRAs and thereby confirmed that RNO8 but not RNO6 of MWF carries genetic variants that contribute to both albuminuria and endothelial dysfunction not only in the aorta (Steireif *et al.*, 2013) but also in mesenteric resistance vessels.

In addition, we demonstrated that albuminuria is associated with arterial stiffness as alterations in increased distensibility, wall stress, strain and β-values found in MWF were completely restored by albuminuria suppression in both consomic MWF-6^{SHR} and MWF-8^{SHR} rats. This correlates with a significantly increased amount of elastin in EEL, although it does not reach WKY levels. However, no influence of the major albuminuria QTL on RNO6 and RNO8 on IEL elastin amount or organization was observed. In addition, MWF exhibited a significant inborn nephron deficit compared with SHR that is in part due to an impairment of early nephrogenesis (Schulte *et al.*, 2012). Nevertheless, this phenotype seems to be independent of arterial stiffness development as arterial elasticity is completely restored in MWF-8^{SHR} rats, although the nephron deficit is unlike MWF-6^{SHR} but similar to MWF in

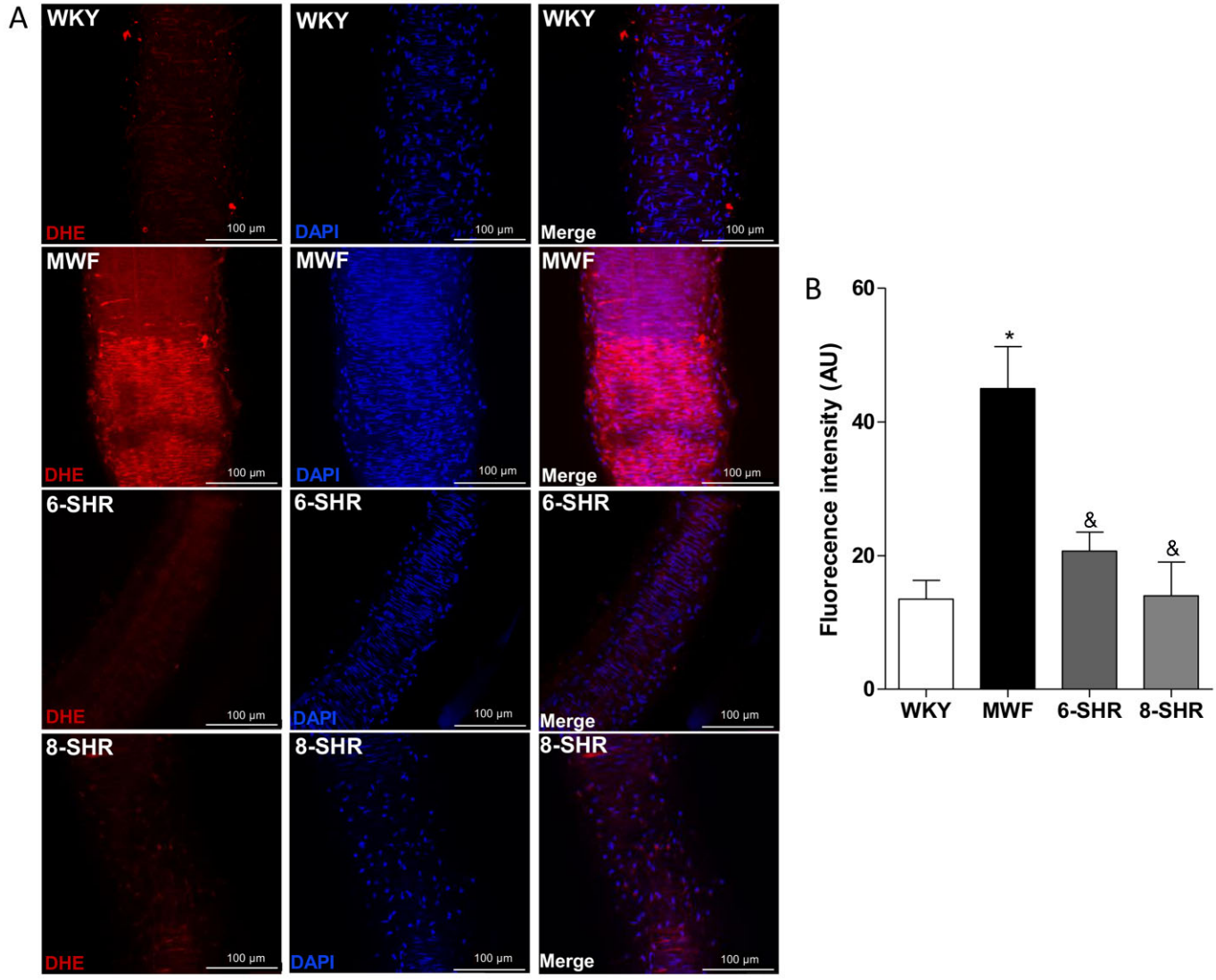

Figure 5

Determination of superoxide anion availability. (A) Representative confocal projections showing *in situ* superoxide generation determined with DHE (3 µM) in MAs from WKY, MWF, MWF-6^{SHR} and MWF-8^{SHR}. Projections were obtained from serial optical sections captured with a fluorescence confocal microscope (×20 oil immersion objective, zoom ×2). (B) Bars show quantification of superoxide anion levels. Results are expressed as mean ± SEM of $n = 5$. *$P < 0.05$ compared with WKY and $^{\&}P < 0.05$ compared with MWF.

this consomic strain (Schulz *et al.*, 2008). Moreover, the observed beneficial effects of the exchange of RNO6 and RNO8 on both albuminuria and arterial stiffness are not secondary to a blood pressure lowering effect, as consomic animals exhibited similar (MWF-6^{SHR}) or even higher levels (MWF-8^{SHR}) compared with MWF. Studies that aim to identify the functional role of candidate genes and to unravel the molecular mechanisms that are affected by the gene loci on RNO6 and RNO8 are currently underway. Nevertheless, comparative mapping analysis indicates that the gene loci do not co-localize with gene loci that have recently been associated with hypertension (Tragante *et al.*, 2014) or arterial stiffness (Mitchell *et al.*, 2012; Beygui *et al.*, 2014) in humans in genome-wide association studies.

Alterations in elastin during development greatly contribute to vascular wall remodelling (Gonzalez *et al.*, 2006). In this context, several cross-sectional studies show an association between albuminuria and a higher carotid intima–media thickness (Rodondi *et al.*, 2007; Kong *et al.*, 2012) and a worse cardiac diastolic function with greater arterial and ventricular end-systolic stiffness (Shah *et al.*, 2011). These studies suggest that the development of cardiovascular remodelling might be another potential mechanism linking increased albuminuria and cardiovascular damage (Schulz *et al.*, 2007; Szymanski *et al.*, 2012). The reduction in cross-sectional area, internal and external diameters found in MRA from MWF without changes in WT are typical features of hypotrophic inward remodelling (Mulvany *et al.*, 1996). As a result of this, the data presented in this study suggest that both vascular remodelling and alterations in elastin content and organization might be associated with the compromised mechanical performance of MRA from MWF. However, despite the fact

that arterial stiffness was restored in both MWF-8^{SHR} and MWF-6^{SHR}, the vascular remodelling observed in MRA from those rats was not ameliorated by introgression of either RNO8 or RNO6 from SHR into MWF. Therefore, these results suggest that the inward hypotrophic remodelling detected in MWF rats is not directly associated with the albuminuria development that is attributable to the QTL on RNO6 or RNO8 respectively. Nevertheless, an effect of other minor albuminuria QTL different from those of RNO6 or RNO8 (Schulz and Kreutz, 2012a) on the development of the vascular remodelling phenotype cannot be excluded. Further experiments are thus necessary to analyse the mechanisms underlying vascular remodelling and how they are associated with the development of albuminuria.

In conclusion, the current study shows that albuminuria development is associated with an increase in arterial stiffness through a reduction in elastin content in the EEL. Moreover, we demonstrated that two major genetic loci linked to albuminuria development (RNO8 and RNO6) affect both albuminuria and arterial stiffness and thus indicate a link between renal injury and compromised mechanical properties of resistant arteries. In addition, although we characterized an inward hypotrophic remodelling phenotype in albuminuric MWF, this finding does not seem to be associated with albuminuria.

Acknowledgements

We acknowledge the contributions of Brigitta Schwaneberg for excellent laboratory assistance, Bettina Bublath and Christiane Priebsch for excellent support in animal breeding and Dolores Morales for her help with the confocal microscope. This study was supported by the Deutsche Hochdruckliga (DHL) Hypertensiologie Professur to R. K., grants from the DFG KR 1152-3-1; DFG SCHU 2604/1-1, SAF2011-25303, GR921641; and Fundación Mutua Madrileña.

Author contributions

M. G.-O. and B. S.: conception and design of the work; acquisition, analysis and interpretation of data; drafting the work and revising it critically for important intellectual content; final approval of the version to be published; agreement to be accountable for all aspects of the work in ensuring that questions related to the accuracy or integrity of any part of the work are appropriately investigated and resolved. R. K.: conception and design of the work, drafting the work and revising it critically for important intellectual content, final approval of the version to be published, agreement to be accountable for all aspects of the work in ensuring that questions related to the accuracy or integrity of any part of the work are appropriately investigated and resolved. M. S. F.-A.: conception and design of the work, analysis and interpretation of data, drafting the work and revising it critically for important intellectual content, final approval of the version to be published, agreement to be accountable for all aspects of the work in ensuring that questions related to the accuracy or integrity of any part of the work are appropriately investigated and resolved. S. A.: conception and design of the work, analysis and interpretation of data, revising the work critically for important intellectual content, final approval of the version to be published, agreement to be accountable for all aspects of the work in ensuring that questions related to the accuracy or integrity of any part of the work are appropriately investigated and resolved. C. F. G.-P., C. S., M. C. G. and A. S.: acquisition, analysis and interpretation of data; drafting the work; final approval of the version to be published; agreement to be accountable for all aspects of the work in ensuring that questions related to the accuracy or integrity of any part of the work are appropriately investigated and resolved. G. R.-H.: interpretation of data, revising the work critically for important intellectual content, final approval of the version to be published, agreement to be accountable for all aspects of the work in ensuring that questions related to the accuracy or integrity of any part of the work are appropriately investigated and resolved.

Conflict of interest

There are no conflicts of interest.

References

Alexander SP, Benson HE, Faccenda E, Pawson AJ, Sharman JL, Spedding M *et al.* (2013a). The concise guide to PHARMACOLOGY 2013/14: enzymes. Br J Pharmacol 170: 1797–1867.

Alexander SP, Benson HE, Faccenda E, Pawson AJ, Sharman JL, Spedding M *et al.* (2013b). The concise guide to PHARMACOLOGY 2013/14: G protein-coupled receptors. Br J Pharmacol 170: 1459–1581.

Arribas SM, Briones AM, Bellingham C, Gonzalez MC, Salaices M, Liu K *et al.* (2008). Heightened aberrant deposition of hard-wearing elastin in conduit arteries of prehypertensive SHR is associated with increased stiffness and inward remodeling. Am J Physiol Heart Circ Physiol 295: H2299–H2307.

Beygui F, Wild PS, Zeller T, Germain M, Castagne R, Lackner KJ *et al.* (2014). Adrenomedullin and arterial stiffness: integrative approach combining monocyte ADM expression, plasma MR-Pro-ADM, and genome-wide association study. Circ Cardiovasc Genet 7: 634–641.

Bouchi R, Babazono T, Mugishima M, Yoshida N, Nyumura I, Toya K *et al.* (2011). Arterial stiffness is associated with incident albuminuria and decreased glomerular filtration rate in type 2 diabetic patients. Diabetes Care 34: 2570–2575.

Briones AM, Gonzalez JM, Somoza B, Giraldo J, Daly CJ, Vila E *et al.* (2003). Role of elastin in spontaneously hypertensive rat small mesenteric artery remodelling. J Physiol 552 (Pt 1): 185–195.

Cerezo C, Ruilope LM, Segura J, Garcia-Donaire JA, de la Cruz JJ, Banegas JR *et al.* (2012). Microalbuminuria breakthrough under chronic renin-angiotensin-aldosterone system suppression. J Hypertens 30: 204–209.

Conde MV, Gonzalez MC, Quintana-Villamandos B, Abderrahim F, Briones AM, Condezo-Hoyos L *et al.* (2011). Liver growth factor treatment restores cell-extracellular matrix balance in resistance

arteries and improves left ventricular hypertrophy in SHR. Am J Physiol Heart Circ Physiol 301: H1153–H1165.

Deckert T, Feldt-Rasmussen B, Borch-Johnsen K, Jensen T, Kofoed-Enevoldsen A (1989). Albuminuria reflects widespread vascular damage. The Steno hypothesis. Diabetologia 32: 219–226.

Divers J, Freedman BI (2010). Susceptibility genes in common complex kidney disease. Curr Opin Nephrol Hypertens 19: 79–84.

Dobrin PB (1978). Mechanical properties of arteries. Physiol Rev 58: 397–460.

Fassi A, Sangalli F, Maffi R, Colombi F, Mohamed EI, Brenner BM *et al*. (1998). Progressive glomerular injury in the MWF rat is predicted by inborn nephron deficit. J Am Soc Nephrol 9: 1399–1406.

Fogarty DG, Rich SS, Hanna L, Warram JH, Krolewski AS (2000). Urinary albumin excretion in families with type 2 diabetes is heritable and genetically correlated to blood pressure. Kidney Int 57: 250–257.

Freedman BI, Bowden DW, Rich SS, Xu J, Wagenknecht LE, Ziegler J *et al*. (2008). Genome-wide linkage scans for renal function and albuminuria in Type 2 diabetes mellitus: the Diabetes Heart Study. Diabet Med 25: 268–276.

Gansevoort RT, Nauta FL, Bakker SJ (2010). Albuminuria: all you need to predict outcomes in chronic kidney disease? Curr Opin Nephrol Hypertens 19: 513–518.

Gil-Ortega M, Condezo-Hoyos L, Garcia-Prieto CF, Arribas SM, Gonzalez MC, Aranguez I *et al*. (2014). Imbalance between pro and anti-oxidant mechanisms in perivascular adipose tissue aggravates long-term high-fat diet-derived endothelial dysfunction. PLoS ONE 9: e95312.

Gonzalez JM, Briones AM, Starcher B, Conde MV, Somoza B, Daly C *et al*. (2005). Influence of elastin on rat small artery mechanical properties. Exp Physiol 90: 463–468.

Gonzalez JM, Briones AM, Somoza B, Daly CJ, Vila E, Starcher B *et al*. (2006). Postnatal alterations in elastic fiber organization precede resistance artery narrowing in SHR. Am J Physiol Heart Circ Physiol 291: H804–H812.

Gonzalez JM, Somoza B, Conde MV, Fernandez-Alfonso MS, Gonzalez MC, Arribas SM (2008). Hypertension increases middle cerebral artery resting tone in spontaneously hypertensive rats: role of tonic vasoactive factor availability. Clin Sci (Lond) 114: 651–659.

Gschwend S, Pinto-Sietsma SJ, Buikema H, Pinto YM, van Gilst WH, Schulz A *et al*. (2002). Impaired coronary endothelial function in a rat model of spontaneous albuminuria. Kidney Int 62: 181–191.

Gschwend S, Haug MB, Nierhaus M, Schulz A, Vetter R, Kossmehl P *et al*. (2009). Short-term treatment with a beta-blocker with vasodilative capacities improves intrarenal endothelial function in experimental renal failure. Life Sci 85: 431–437.

Hashimoto J, Ito S (2011). Central pulse pressure and aortic stiffness determine renal hemodynamics: pathophysiological implication for microalbuminuria in hypertension. Hypertension 58: 839–846.

Hermans MM, Henry R, Dekker JM, Kooman JP, Kostense PJ, Nijpels G *et al*. (2007). Estimated glomerular filtration rate and urinary albumin excretion are independently associated with greater arterial stiffness: the Hoorn Study. J Am Soc Nephrol 18: 1942–1952.

Hermans MM, Henry RM, Dekker JM, Nijpels G, Heine RJ, Stehouwer CD (2008). Albuminuria, but not estimated glomerular filtration rate, is associated with maladaptive arterial remodeling: the Hoorn Study. J Hypertens 26: 791–797.

Huang L, Zhang S, Liu D, Yan X, Yan S (2014). Low-grade albuminuria associated with brachial-ankle pulse wave velocity in younger adults with type 2 diabetes mellitus in China. Diabetes Metab Res Rev 31: 262–268.

Intengan HD, Thibault G, Li JS, Schiffrin EL (1999). Resistance artery mechanics, structure, and extracellular components in spontaneously hypertensive rats: effects of angiotensin receptor antagonism and converting enzyme inhibition. Circulation 100: 2267–2275.

Ishikawa T, Hashimoto J, Morito RH, Hanazawa T, Aikawa T, Hara A *et al*. (2008). Association of microalbuminuria with brachial-ankle pulse wave velocity: the Ohasama study. Am J Hypertens 21: 413–418.

Kilkenny C, Browne W, Cuthill IC, Emerson M, Altman DG (2010). Animal research: reporting in vivo experiments: the ARRIVE guidelines. Br J Pharmacol 160: 1577–1579.

Kim BJ, Lee HA, Kim NH, Kim MW, Kim BS, Kang JH (2011). The association of albuminuria, arterial stiffness, and blood pressure status in nondiabetic, nonhypertensive individuals. J Hypertens 29: 2091–2098.

Kohara K, Tabara Y, Tachibana R, Nakura J, Miki T (2004). Microalbuminuria and arterial stiffness in a general population: the Shimanami Health Promoting Program (J-SHIPP) study. Hypertens Res 27: 471–477.

Kong X, Jia X, Wei Y, Cui M, Wang Z, Tang L *et al*. (2012). Association between microalbuminuria and subclinical atherosclerosis evaluated by carotid artery intima-media in elderly patients with normal renal function. BMC Nephrol 13: 37.

Kreutz R, Kovacevic L, Schulz A, Rothermund L, Ketteler M, Paul M (2000). Effect of high NaCl diet on spontaneous hypertension in a genetic rat model with reduced nephron number. J Hypertens 18: 777–782.

Krolewski AS, Poznik GD, Placha G, Canani L, Dunn J, Walker W *et al*. (2006). A genome-wide linkage scan for genes controlling variation in urinary albumin excretion in type II diabetes. Kidney Int 69: 129–136.

Matsushita K, van der Velde M, Astor BC, Woodward M, Levey AS, de Jong PE *et al*. (2010). Association of estimated glomerular filtration rate and albuminuria with all-cause and cardiovascular mortality in general population cohorts: a collaborative meta-analysis. Lancet 375: 2073–2081.

McGrath JC, Drummond GB, McLachlan EM, Kilkenny C, Wainwright CL (2010). Guidelines for reporting experiments involving animals: the ARRIVE guidelines. Br J Pharmacol 160: 1573–1576.

Mitchell GF, Verwoert GC, Tarasov KV, Isaacs A, Smith AV, Yasmin *et al*. (2012). Common genetic variation in the 3′-BCL11B gene desert is associated with carotid-femoral pulse wave velocity and excess cardiovascular disease risk: the AortaGen Consortium. Circ Cardiovasc Genet 5: 81–90.

Mottl AK, Vupputuri S, Cole SA, Almasy L, Goring HH, Diego VP *et al*. (2009). Linkage analysis of albuminuria. J Am Soc Nephrol 20: 1597–1606.

Mule G, Cottone S, Vadala A, Volpe V, Mezzatesta G, Mongiovi R *et al*. (2004). Relationship between albumin excretion rate and aortic stiffness in untreated essential hypertensive patients. J Intern Med 256: 22–29.

Mulvany MJ, Baumbach GL, Aalkjaer C, Heagerty AM, Korsgaard N, Schiffrin EL *et al*. (1996). Vascular remodeling. Hypertension 28: 505–506.

Munakata M, Miura Y, Yoshinaga K (2009). Higher brachial-ankle pulse wave velocity as an independent risk factor for future microalbuminuria in patients with essential hypertension: the J-TOPP study. J Hypertens 27: 1466–1471.

Pawson AJ, Sharman JL, Benson HE, Faccenda E, Alexander SP, Buneman OP *et al*.; NC-IUPHAR (2014). The IUPHAR/BPS Guide to PHARMACOLOGY: an expert-driven knowledgebase of drug targets and their ligands. Nucl Acids Res 42 (Database Issue): D1098–D1106.

Rodondi N, Yerly P, Gabriel A, Riesen WF, Burnier M, Paccaud F *et al*. (2007). Microalbuminuria, but not cystatin C, is associated with carotid atherosclerosis in middle-aged adults. Nephrol Dial Transplant 22: 1107–1114.

Ruiz-Hurtado G, Condezo-Hoyos L, Pulido-Olmo H, Aranguez I, Del Carmen Gonzalez M, Arribas S *et al*. (2014). Development of albuminuria and enhancement of oxidative stress during chronic renin-angiotensin system suppression. J Hypertens 32: 2082–2091.

Satoh M (2012). Endothelial dysfunction as an underlying pathophysiological condition of chronic kidney disease. Clin Exp Nephrol 16: 518–521.

Schiffrin EL, Lipman ML, Mann JF (2007). Chronic kidney disease: effects on the cardiovascular system. Circulation 116: 85–97.

Schulte L, Schulz A, Unland J, Schulz H, Hubner N, Schmidt-Ott KM *et al*. (2012). MWF rats with spontaneous albuminuria inherit a reduced efficiency of nephron induction during early nephrogenesis in comparison to SHR rats. J Hypertens 30: 2031–2038.

Schulz A, Kreutz R (2012a). Mapping genetic determinants of kidney damage in rat models. Hypertens Res 35: 675–694.

Schulz A, Litfin A, Kossmehl P, Kreutz R (2002). Genetic dissection of increased urinary albumin excretion in the Munich Wistar Fromter rat. J Am Soc Nephrol 13: 2706–2714.

Schulz A, Standke D, Kovacevic L, Mostler M, Kossmehl P, Stoll M *et al*. (2003). A major gene locus links early onset albuminuria with renal interstitial fibrosis in the MWF rat with polygenetic albuminuria. J Am Soc Nephrol 14: 3081–3089.

Schulz A, Weiss J, Schlesener M, Hansch J, Wehland M, Wendt N *et al*. (2007). Development of overt proteinuria in the Munich Wistar Fromter rat is suppressed by replacement of chromosome 6 in a consomic rat strain. J Am Soc Nephrol 18: 113–121.

Schulz A, Hansch J, Kuhn K, Schlesener M, Kossmehl P, Nyengaard JR *et al*. (2008). Nephron deficit is not required for progressive proteinuria development in the Munich Wistar Fromter rat. Physiol Genomics 35: 30–35.

Schulz A, Schutten-Faber S, van Es N, Unland J, Schulte L, Kossmehl P *et al*. (2012b). Induction of albuminuria and kidney damage in SHR by transfer of chromosome 8 from Munich Wistar Fromter rats. Physiol Genomics 44: 110–116.

Shah AM, Lam CS, Cheng S, Verma A, Desai AS, Rocha RA *et al*. (2011). The relationship between renal impairment and left ventricular structure, function, and ventricular-arterial interaction in hypertension. J Hypertens 29: 1829–1836.

Sjoblom P, Nystrom FH, Lanne T, Engvall J, Ostgren CJ (2014). Microalbuminuria, but not reduced eGFR, is associated with cardiovascular subclinical organ damage in type 2 diabetes. Diabetes Metab 40: 49–55.

Smith A, Karalliedde J, De Angelis L, Goldsmith D, Viberti G (2005). Aortic pulse wave velocity and albuminuria in patients with type 2 diabetes. J Am Soc Nephrol 16: 1069–1075.

Steireif C, Garcia-Prieto CF, Ruiz-Hurtado G, Pulido-Olmo H, Aranguez I, Gil-Ortega M *et al*. (2013). Dissecting the genetic predisposition to albuminuria and endothelial dysfunction in a genetic rat model. J Hypertens 31: 2203–2212.

Szymanski MK, Buikema JH, van Veldhuisen DJ, Koster J, van der Velden J, Hamdani N *et al*. (2012). Increased cardiovascular risk in rats with primary renal dysfunction; mediating role for vascular endothelial function. Basic Res Cardiol 107: 242.

Tragante V, Barnes MR, Ganesh SK, Lanktree MB, Guo W, Franceschini N *et al*. (2014). Gene-centric meta-analysis in 87,736 individuals of European ancestry identifies multiple blood-pressure-related loci. Am J Hum Genet 94: 349–360.

Ulu N, Schoemaker RG, Henning RH, Buikema H, Teerlink T, Zijlstra FJ *et al*. (2009). Proteinuria-associated endothelial dysfunction is strain dependent. Am J Nephrol 30: 209–217.

Vaziri ND, Ni Z, Oveisi F, Liang K, Pandian R (2002). Enhanced nitric oxide inactivation and protein nitration by reactive oxygen species in renal insufficiency. Hypertension 39: 135–141.

Wilkinson IB, Qasem A, McEniery CM, Webb DJ, Avolio AP, Cockcroft JR (2002). Nitric oxide regulates local arterial distensibility in vivo. Circulation 105: 213–217.

Yokoyama H, Aoki T, Imahori M, Kuramitsu M (2004). Subclinical atherosclerosis is increased in type 2 diabetic patients with microalbuminuria evaluated by intima-media thickness and pulse wave velocity. Kidney Int 66: 448–454.

Supporting information

Additional Supporting Information may be found in the online version of this article at the publisher's web-site:

http://dx.doi.org/10.1111/bph.13223

Figure S1 Characterization of endothelial function in an organ bath and endothelial factor contribution to ACh-induced relaxation. (A) Cumulative concentration–response curves to ACh (10^{-9}–10^{-4} mol·L^{-1}) in MA from MWF and SHR. Data are means ± SEM (n = 5 animals per group). (B) Effect of L-NAME (10^{-4} M) on ACh-induced relaxation in mesenteric arteries from SHR. ***P < 0.001 compared with control relaxation. Data are means ± SEM (n = 5 animals per group).

Figure S2 Characterization of structural parameters by pressure myography. (A) External diameter–pressure, (B) internal diameter–pressure, (C) WT–pressure, (D) wall-to-lumen ratio–pressure and (E) and cross-sectional area–pressure curves in MA from MWF and SHR incubated in Ca^{2+}-free KH. Results are expressed as mean ± SEM of n = 5 for MWF and n = 6 for SHR. *P < 0.05, **P < 0.01 compared with SHR.

Figure S3 Characterization of mechanical parameters by pressure myography. (A) Incremental distensibility–pressure curve, (B) wall stress–pressure curve, (C) strain–pressure curve and (D) stress–strain relationships with β-values obtained from fully relaxed (Ca^{2+}-free KH) MA segments from MWF and SHR calculated from pressure myography data. Data are expressed as mean ± SEM of n = 5 for MWF and n = 6 for SHR. ***P < 0.001 compared with SHR.

Figure S4 Determination of elastin content and organization. Representative confocal projections of the EEL (A) and IEL (B) of MA from MWF and SHR. Projections were obtained from serial optical sections captured with a fluorescence con-

focal microscope (×63 oil immersion objective, zoom ×2). Diagram bars show quantification of elastin proportion in EEL (C) and elastin content in IEL (D), fenestrae size (E) and fenestrae number (F). Results are expressed as mean ± SEM of $n = 5$. *$P < 0.05$ and **$P < 0.01$ compared with SHR.

Figure S5 Determination of superoxide anion availability. (A) Representative confocal projections showing *in situ* superoxide generation determined with DHE (3 μM) in MAs from MWF and SHR. Projections were obtained from serial optical sections captured with a fluorescence confocal microscope (×20 oil immersion objective, zoom ×2). (B) Diagram bars show quantification of superoxide anion levels. Results are expressed as mean ± SEM of $n = 5$.